[CANCER RESEARCH 61, 4550–4555, June 1, 2001]

# Apoptotic Triggers Initiate Translocations within the *MLL* Gene Involving the Nonhomologous End Joining Repair System[1]

**Christopher J. Betti,[2] Michael J. Villalobos,[2] Manuel O. Diaz, and Andrew T. M. Vaughan[3]**

*Program in Molecular Biology [C. J. B., M. J. V.], Departments of Radiation Oncology [A. T. M. V.] and Medicine [M. O. D.], Loyola University Medical Center, Maywood, Illinois 60153*

## ABSTRACT

**Translocations involving the *MLL* gene at 11q23 are a frequent finding in therapy-related leukemia and are concentrated within a short, 8.3-kb tract of DNA, the breakpoint cluster region. In addition, a specific site adjacent to exon 12 within this region of *MLL* is cleaved in cells undergoing apoptosis. We show here, using human TK6 lymphoblastoid cells, that irradiation and the apoptotic trigger anti-CD95 antibody are each able to initiate translocations at the *MLL* exon 12 cleavage site. The translocation junctions produced contain regions of microhomology consistent with operation of the nonhomologous end joining (NHEJ) repair process. Participation of the NHEJ process is supported by the identification of the NHEJ component DNA-PKcs at the site of apoptotic cleavage. Suppression of DNA-PKcs function by the phosphatidylinositol 3-kinase inhibitor wortmannin compromises DNA end joining, increases site-specific cleavage within *MLL*, and eliminates *MLL*-restricted translocations. We propose that activation of apoptotic effector nucleases alone is sufficient to generate proleukemogenic translocations and raises the possibility that some of these may persist in cells that evade apoptotic execution and survive.**

## INTRODUCTION

Translocations involving the *MLL* gene are a frequent finding in infant and adult acute leukemias and are also observed in therapy-related leukemias (1). Numerous chromosomal partners have been described to be associated with the 11q23 region, suggesting that loss of *MLL* function(s) contributes to the critical leukemogenic lesion (2). No single mechanism has been proposed that is able to explain all observed translocations within *MLL*. The activation of host V(D)J recombinase has been suggested as a mediator of translocations (3). This interpretation has been questioned, however, in that the required heptamer and nonamer recombination target sequences were not found in many t(4;11) translocations, one of the most frequent types of *MLL* aberrations observed (4). Alternatively, repeated tracts of DNA, such as Alu repeats, may provide less restricted targets for homologous recombination, resulting in a translocation (5). Drugs that are inhibitors of DNA topoisomerase II, including etoposide, have also been implicated as the causative agent in therapy-related leukemia, and this argument is supported by the proximity of a topoisomerase II consensus sequence within a region of *MLL* that is subject to frequent translocations (6, 7). The diversity of possible mechanisms suggests that multiple factors may impact the translocation process, and the type of event observed may depend on both the target cell and initiating insult. It has recently been shown, as might be expected, that the introduction of two DNA double-strand breaks into cells provides a potent initiator of translocation between these two sites (8). Once such breaks are created at a potential translocation target site, they will immediately be subject to attempts at repair through the NHEJ[4] system (9). Failure of this repair process to operate correctly has been suggested as a mediator of translocation events by the signature regions of microhomology left at the translocation junctions in human leukemia (2). In contrast to lower organisms such as yeast that utilize homologous recombination, the NHEJ pathway is the principal mechanism whereby mammalian cells repair DNA double-strand breaks (9–13). These may be breaks introduced by external agents, including ionizing radiation and cytotoxic drugs, or those arising from normal biological processes such as V(D)J recombination (14). Successful execution of NHEJ repair requires the binding of the Ku70/Ku80 heterodimer to both broken DNA ends, followed by the recruitment of the catalytic subunit DNA-PKcs, DNA ligase IV, and Xrcc4 (15). In the therapy-related translocations observed in *MLL*, the chromosomal breakpoints are clustered within the 3′ side of an 8.3-kb tract of DNA, the BCR, the same region that has been shown to be cleaved by nucleases of the apoptotic effector pathway (6, 16, 17). We were interested in addressing the very earliest steps in leukemogenesis and asked whether the initiating translocation break might be linked mechanistically to inappropriate activation of the apoptotic effector machinery. In this case, activation of the apoptotic nuclease(s) would create a break within the *MLL* gene that may be joined to a partner chromosome.

## MATERIALS AND METHODS

**Analysis of *MLL* BCR Rejoining.** Apoptosis was induced in human lymphoblastoid TK6 cells by exposure to 8 Gy of γ-radiation (Cs-137) and confirmed by propidium iodide staining (0.5 μg/ml) and inspection of nuclear morphology. Wortmannin was added 4 h after irradiation to allow the repair of radiation-induced DNA breaks. DNA was isolated from TK6 cells at various times after irradiation and subjected to digestion with *Bam*HI. A Southern blot was performed using a 0.74-kb cDNA probe to the *MLL* BCR as reported by others (7).

**Detection of DNA-PKcs Cleavage.** Cell extracts were prepared from TK6 cells at various times after apoptotic induction. Electrophoresis was performed on 50 μg of protein sample using 7.5% SDS-PAGE gels. Proteins were transferred to polyvinylidene difluoride membranes (Bio-Rad, Hercules, CA), and immunoblotting was performed using a monoclonal antibody to human DNA-PKcs (Oncogene Research Products, Cambridge, MA).

**Chromatin Immunoprecipitation of DNA-PKcs Linked to *MLL*.** TK6 cells were irradiated with 8 Gy of γ-radiation and harvested at 6 and 24 h after exposure. Subsequently, formaldehyde was added directly to cell culture media to a final concentration of 1%. Procedures followed were as described previously, except that protein A/G-agarose was substituted for lyophilized Staph A cells (18). Immunoprecipitation was performed with 1 μg of mouse monoclonal antihuman DNA-PKcs antibody (Oncogene Research Products). DNA selected by this approach was analyzed for *MLL*-restricted sequences by PCR using primers 5′-AGGAC-AAACC-AGACC-TTACA-AC-3′ and 5′-GCTCG-TTCTC-CTCTA-AACAA-AA-3′.

**Translocation Analysis by IPCR.** Genomic DNA was extracted from TK6 cell cultures after 8 Gy of γ-radiation. DNA (6 μg) was digested with either *Sau*3AI or a combination of *Sau*3AI and *Xba*I. The addition of *Xba*I will

Received 11/29/00; accepted 4/3/01.

The costs of publication of this article were defrayed in part by the payment of page charges. This article must therefore be hereby marked *advertisement* in accordance with 18 U.S.C. Section 1734 solely to indicate this fact.

[1] This work was supported in part by generous financial support from the Wolf family.

[2] C. J. B. and M. J. V. contributed equally to this work.

[3] To whom requests for reprints should be addressed, at Loyola University Medical Center, Cardinal Bernadin Cancer Center, Room 338, 2160 South First Avenue, Maywood, IL 60153.

[4] The abbreviations used are: NHEJ, nonhomologous end joining; BCR, break point cluster region; IPCR, inverse PCR; CAD, caspase-activated deoxyribonuclease; ICAD, inhibitor of CAD; LINE, long interspersed nucleotide element.

eliminate amplification of native *MLL* but allow detection of translocation products that lack an *Xba*I recognition sequence. After digestion, each sample was heat-inactivated at 70°C for 15 min, ethanol-precipitated, and resuspended in water. Ligation with 0.05 unit of T4 ligase was carried out in a final volume of 200 μl with the addition of spermidine (2.5 mM, final concentration) and allowed to proceed for 48 h at 14°C. After ligation, T4 was heat-inactivated at 70°C for a period of 10 min. Individual samples were precipitated in 100% ethanol and resuspended in 30 μl of water. Forty ng of DNA were used in each PCR reaction. PCR was conducted as described previously (19). Two sets of nested primers were used to examine both the intron 11 control region and the exon 12 apoptotic cleavage site. Both sets were used identically for 28 cycles in the first round and 18 cycles in the second round at PCR reaction temperatures of 95°C/55°C/72°C for 1 min/step. The regions analyzed are diagrammed in Fig. 1, and the primers used are shown below.

For intron 11, we used the following primers: forward 1, 5′-ATGTCCATGACATATCACTG-3′; reverse 1, 5′-TAGGACTTCATATTTGCCA-3′; forward 2, 5′-AGCACAATCCCATCTTAGT-3′; and reverse 2, 5′-TGAGACGGAGTCTTGCT-3′. For exon 12, we used the following primers: forward 1, 5′-CTTTGTTTATACCACTC-3′; reverse 1, 5′-TATGGGAATATAAAGGAGTGGG-3′; forward 2, 5′-TTAGGTCACTTAGCATGTTCTG-3′; and reverse 2, 5′-CAGTTGTAAGGTCTGGTTTGTC-3′.

PCR products were subsequently separated by gel electrophoresis. The presence of specific MLL sequences within each amplified product was determined by Southern blotting as follows. For the detection of *MLL* within exon 12, the 0.74-kb cDNA probe as reported by Strissel *et al.* (7) was used.

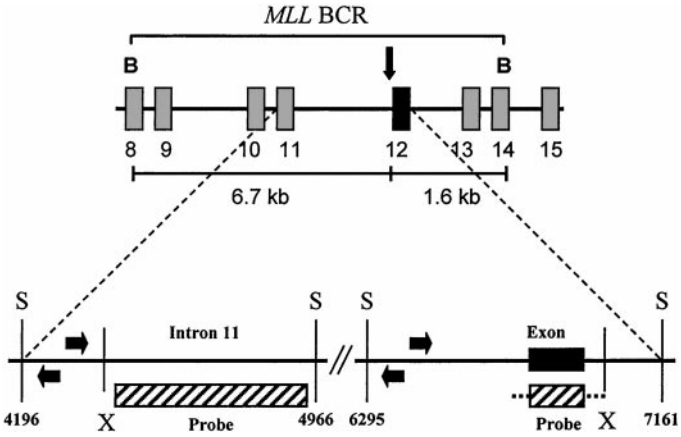


Fig. 1. *MLL* BCR. The exon structure of the *MLL* breakpoint region is shown. The *vertical arrow* indicates the approximate target for apoptotic cleavage and the *MLL* fragment sizes produced. The *bottom diagram* indicates the region for IPCR analysis, with *horizontal arrows* indicating the approximate starting location for initial primer binding in control DNA (*left*) or the apoptotic target location (*right*). Hybridization probes used include a cDNA for the complete BCR and an intronic probe for the control region as shown. *B*, *Bam*H1 restriction sites defining the BCR; *S*, *Sau*3AI cut sites for creating the IPCR templates; *X*, *Xba*I cut site used to eliminate amplification of germ-line *MLL* sequences. Nucleotide numbering of the 8.3-kb BCR follows the scheme reported by Gu *et al.* (33).

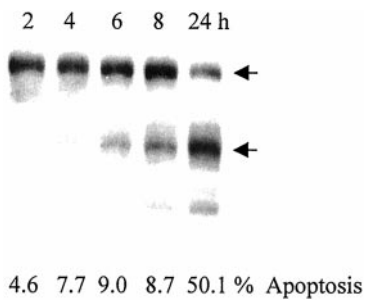


Fig. 2. Cleavage of DNA-PKcs after triggering apoptosis with irradiation. TK6 cells were irradiated with 8 Gy of γ-radiation and analyzed by Western blot for the presence of DNA-PKcs. Cleavage was detected 6 h after irradiation, but at both 8 and 24 h after irradiation, native DNA-PKcs is still detectable. *Top arrow*, DNA-PKcs; *bottom arrow*, cleavage product. Also shown is the percentage of apoptotic cells at each time point as measured by nuclear morphology.

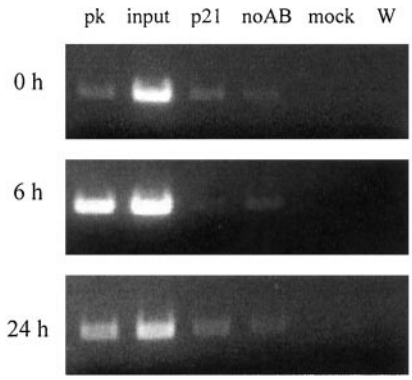


Fig. 3. Association of DNA-PKcs and *MLL* in TK6 cells irradiated with 8 Gy. Each of the three panels shows a 441-bp PCR fragment amplified from *MLL* sequence immediately 5′ from the *MLL* cleavage site. Input DNA reflects PCR amplification from genomic DNA before selection by immunoprecipitation. Immunoprecipitation using anti-DNA-PKcs antibody (+*PK*) without irradiation, control antibody to p21 (+*p21*), and no antibody (*No Ab*) each gave a faint signal, beads alone (*mock*) and the water control for PCR (*W*) were both negative. At both 6 and 24 h after irradiation, a strong signal was observed from the material precipitated with anti-DNA-PKcs, indicating that DNA-PKcs accumulates at the *MLL* breakpoint after irradiation.

For the identification of intronic *MLL* sequences within the control IPCR region, a probe was constructed by excising a 0.82-kb *MLL* intronic fragment after *Eco*RV and *Xba*1 cleavage of a plasmid containing the genomic 8.3-kb BCR of *MLL*. The fragment required was separated on a DNA gel, extracted, and subsequently radiolabeled using standard methods.

**Translocation Sequence Analysis.** Individual IPCR products were extracted from DNA gels, using samples treated with *Xba*1 to minimize MLL germ-line cloning, from both the 8 h time point after irradiation and the 6 h time point after anti-CD95 treatment. These products were then cloned into the pCR4-TOPO cloning vector (Invitrogen, Carlsbad, CA), selected on plates containing 50 μg/ml ampicillin according to the manufacturer's instructions, expanded in liquid culture, and sequenced. DNA sequences obtained were searched against the National Center for Biotechnology Information database,[5] and those providing a match to the input DNA sequence and containing *MLL* were selected and analyzed (Table 1). The boxed areas show regions of microhomology between *MLL* and translocation partner DNA and include the *MLL* breakpoint except for the translocation to a L1 LINE. In the latter case, the breakpoint is 1 base outside the region of homology. Translocation to repetitive DNA, such as LINES, precluded an unambiguous chromosome assignment.

## RESULTS AND DISCUSSION

In this study, we were specifically interested in the fate of DNA double-strand breaks introduced at the *MLL* gene BCR in cell populations exposed to apoptotic triggers (Fig. 1). According to the current interpretation of apoptosis, DNA cleavage is a late but regulated event characteristic of dying cells (20). However, recent evidence has questioned this viewpoint, suggesting that the irreversible commitment to apoptosis may occur after the detection of conventional indicators of apoptosis (21, 22). Thus, membrane inversion of phosphatidyl serine moieties detected by annexin V staining and the introduction of DNA breaks with free 3′ OH termini measured by terminal deoxynucleotidyl transferase-mediated nick end labeling staining have both been linked to viable, nonapoptotic cells (21, 22). We were interested in determining whether DNA breaks introduced by the apoptotic process had the potential to be rejoined. The repair-associated proteins DNA-PKcs and poly(ADP-ribose) polymerase are normally subject to caspase 3-mediated cleavage during apoptosis, leading to their inactivation and suppression of DNA repair (20). It was therefore important to determine whether sufficient DNA-PKcs remains after exposure to apoptotic triggers to participate in the NHEJ repair process. As

[5] http://www.ncbi.nlm.nih.gov/BLAST/.

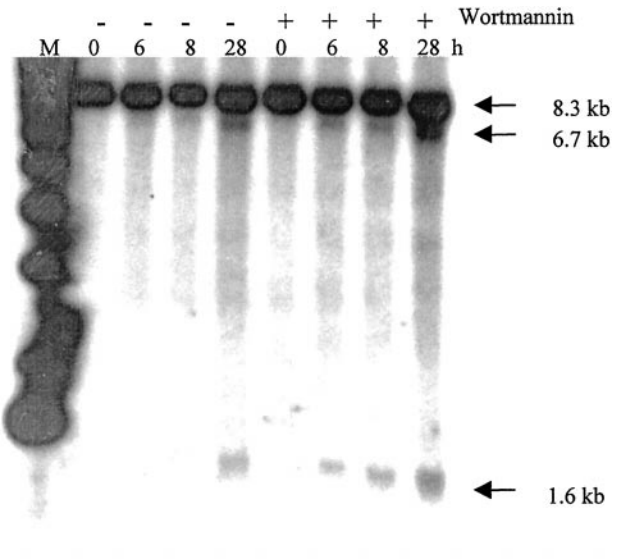


Fig. 4. Southern blot of *MLL* site-specific fragmentation after irradiation with 8 Gy of γ-radiation. After irradiation, site-specific cleavage adjacent to exon 12 is observed as two fragments of 6.7 and 1.6 kb. Addition of the DNA-PKcs inhibitor wortmannin (+) 4 h after irradiation, when repair of the radiation associated breaks is complete, shows increased fragmentation consistent with inhibition of an active DNA repair process at the site of apoptotic cleavage at the *MLL* breakpoint.

shown by Western blotting in Fig. 2, caspase-3-dependent cleavage of the DNA-PKcs protein is detected 6 h after irradiation, but substantial cleavage is only observed after 24 h. At this time, substantial degradation of DNA-PKcs is apparent, leaving approximately 40% of the native form of the protein at a time when approximately 50% of the cells are undergoing apoptosis. To determine whether this level of DNA-PKcs was sufficient to bind broken DNA at the *MLL* cleavage site, DNA bound to DNA-PKcs was isolated using a chromatin immunoprecipitation assay. With this technique, PCR primers were designed to amplify a region of *MLL* DNA approximately 400 bp 5′ of the cut site region within *MLL*. A PCR product is only obtained if the DNA isolated by anti-DNA-PKcs immunoprecipitation contains this *MLL* region physically attached to DNA-PKcs. Using this assay, anti-DNA-PKcs antibody did not precipitate *MLL* sequences from control cells beyond background levels; however, DNA-PKcs was bound to this *MLL* region both 6 and 24 h after triggering apoptosis (Fig. 3). These data indicate that the DNA-PKcs component of the NHEJ complex is recruited to the *MLL* cut site location for at least 24 h after irradiation.

To address the functional activity of DNA repair at the *MLL* apoptotic cleavage site, the BCR of *MLL* was isolated using *Bam*H1 digestion, and the presence of unique fragments indicating site-specific cleavage was detected with a 0.74-kb cDNA *MLL*-specific probe (7). The complete 8.3-kb *MLL* BCR is observed in untreated cells; after irradiation, this is cleaved into 1.6- and 6.7-kb fragments. To observe the effects of DNA repair at this cleavage site, irradiated cells were exposed to the DNA-PKcs inhibitor wortmannin 4 h after irradiation was complete. In a variety of systems, this reagent has been shown to effectively inhibit the rejoining of DNA double-strand breaks (15, 23, 24). The delay in drug administration was designed to allow the DNA double-strand breaks produced by irradiation to be rejoined (15). As shown in Fig. 4, adding wortmannin to cells 4 h after irradiation increased the apoptosis-specific fragmentation of *MLL* DNA sequences, whereas addition of the drug alone had no effect. These data suggest that the *MLL* breakpoint cleaved during apoptosis is subject to DNA-PKcs-dependent NHEJ repair that is suppressed by the presence of wortmannin. Therefore, the inhibition of NHEJ repair increases the total amount of fragmentation observed.

One of several possible consequences of a DNA religation process operating at the *MLL* cleavage site is the potential for misrepair, resulting in a translocation. To detect such events, an IPCR strategy was used (19). In this procedure, the proposed region of translocation is excised by restriction digest, circularized, and amplified using divergent *MLL* primers located on the 5′ side of the proposed cut site (Fig. 1). The experiment was carried out using both primers amplifying sequences adjacent to the cut site location and, as a control, sequences approximately 2 kb centromeric to the target site within intron 11, where no site-specific cleavage is expected. After exposure of TK6 cells to 8 Gy of γ-rays, surviving cells repopulated the culture to preirradiation levels in 7–10 days. Amplification of the control region (intron 11) after irradiation and DNA gel analysis shows a single intense band at 605 bp produced by amplification of germ-line *MLL* sequences (Fig 5*A*). No additional bands are seen, indicating that only the IPCR construct containing *MLL* is present. Examination of potential translocations within the BCR of exon 12, however, shows multiple bands of different sizes in addition to that expected from amplification of germ-line *MLL* sequences (Fig. 5*B*). These are particularly prominent in the lanes treated with *Xba*I, which eliminates amplification of germ-line *MLL* sequences, indicating that transloca-

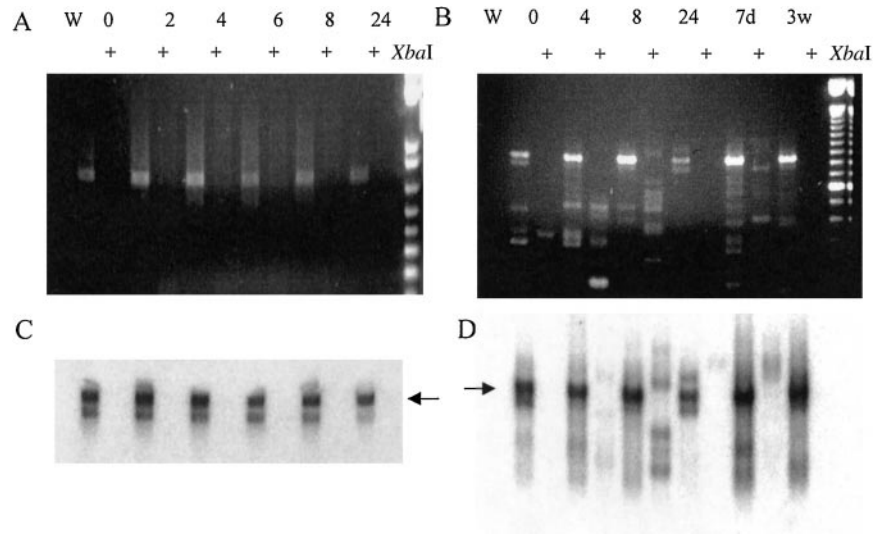


Fig. 5. Translocation events initiated after 8 Gy of γ-radiation within *MLL* identified by the IPCR. *A*, DNA gel of IPCR products examined up to 24 h after irradiation, using primers to the control region. No products other than germ-line (605-bp) *MLL* amplification product are observed. *B*, DNA gel of IPCR products targeting the apoptotic cleavage region, analyzed for up to 3 weeks after irradiation. Amplification of the germ-line *MLL* (702-bp) product is observed with the addition of other products potentially resulting from translocation events that persist from 8 h to 7 days after irradiation. *C* and *D*, Southern blots of the DNA gels shown above using either an intronic probe (*C*; see Fig. 1) or the same 0.74-kb cDNA probe used in Fig. 4 (*D*). In both cases, the predominant products result from the amplification of germ-line *MLL* (*arrows*). *D*, *MLL* containing products that have lost an *Xba*I site, presumably by translocation to foreign DNA, are only observed after IPCR analysis of the region adjacent to the site of apoptotic cleavage. *Lanes* marked with an + contain DNA restricted with *Xba*1, those marked *W* are PCR water controls.

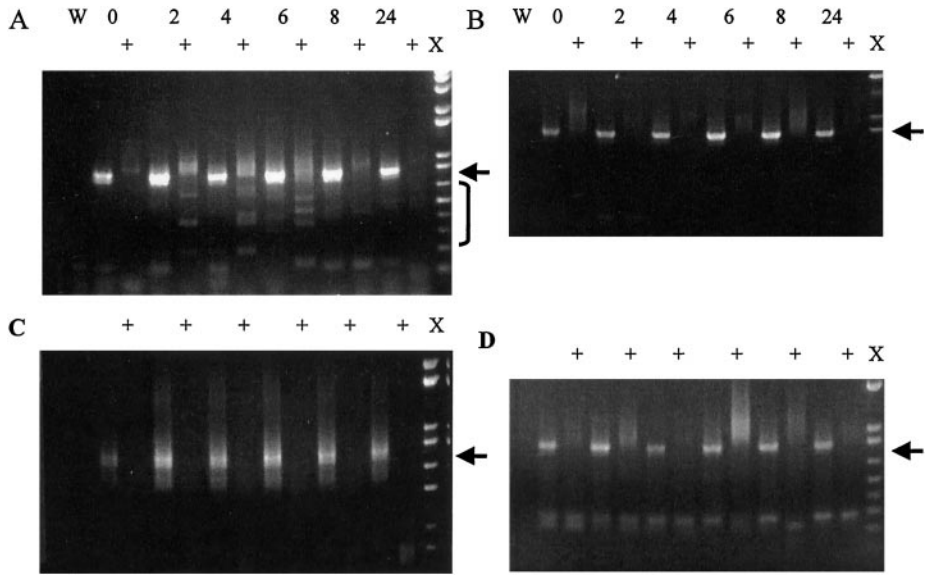


Fig. 6. Modulation of translocation initiated within *MLL* identified by IPCR. *A*, DNA gel of IPCR products produced after triggering apoptosis with 0.5 $\mu$g/ml non-genotoxic anti-CD95 antibody. Potential translocation products are observed in those lanes shown by the *bracket*, where *Xba*I (+) has disrupted amplification of germ-line *MLL*. *B*, addition of the DNA-PKcs inhibitor wortmannin to cells immediately after exposure to 8 Gy of $\gamma$-radiation, no PCR products indicative of translocations are observed (contrast with Fig. 5*B*). *C*, IPCR using primers directed to the control region of intron 11 after exposure to anti-CD95; only the germ-line *MLL* product is observed. *D*, IPCR analysis of p53 mutant, apoptosis-resistant WI-L2-NS cells after exposure to 8 Gy of irradiation; only amplification of germ-line *MLL* is observed (26). *Arrows* point to the product of germ-line *MLL* amplification. *Lanes* marked with an *X* contain DNA restricted with *Xba*1, those marked *W* are PCR water controls.

tions had occurred linking the *MLL* cleavage site to a DNA sequence that lacks an *Xba*I recognition site. To confirm that the bands observed contain *MLL*-specific sequences, a Southern blot analysis using *MLL* probes specific for either intron 11 or exon 12 was performed. These data supported the interpretation made from the DNA gel data and indicated that some of the novel bands obtained 8 and 24 h and 7 days after irradiation contained *MLL* (Fig 5, *C* and *D*). Not all bands observed on the DNA gel were detectable by Southern blotting. This is because some bands contain only short fragments of *MLL*-derived DNA, which presents a weak target for hybridization. Also, a substantial fraction of translocations may occur within intronic regions of *MLL*, and the cDNA probe used cannot detect these. These presumed translocations persist within the irradiated expanding population for up to a week as the treated population returns to preirradiation levels but fade beyond detection by 3 weeks. This would be expected because the majority of cells with translocations will have genetic damage that is inconsistent with long-term growth.

To separate the possibly confounding genotoxic effect of ionizing radiation from its activation of the apoptotic program, the TK6 cells were also exposed to anti-CD95 antibody, a nongenotoxic activator of apoptosis (25). As seen after irradiation, incubation with anti-CD95 antibody generated PCR products consistent with the production of translocations involving the apoptotic hot spot in exon 12 (Fig. 6*A*) but not the control region in intron 11 (Fig. 6*C*). These are therefore translocation events induced only as a consequence of activating the apoptotic program. To confirm the possible mechanism whereby these translocations are produced, the experiment was repeated using irradiation as the apoptotic trigger in the presence of the DNA-PKcs inhibitor wortmannin. As used here, wortmannin is a potent inhibitor of DNA-PKcs and therefore the NHEJ repair process (15). Under these conditions, no translocation-associated PCR products were observed, implying that the NHEJ process was involved in their creation (Fig. 6*B*). A potentially controversial aspect of these experiments is the role of the apoptotic cleavage system in the genesis of *MLL*-specific translocations. To address this specific question, an additional experiment was carried out using a cell line, WI-L2-NS, that shares the same genetic background as TK6 but contains a mutated *p53* gene. We have shown previously that this mutation severely reduces radiation-induced apoptosis (26). After exposure to 8 Gy of $\gamma$-radiation, no translocations were observed in WI-L2-NS using IPCR, suggesting that the genotoxic insult itself was not the source for the observed translocations and that they arise only after activation of the p53-dependent apoptosis machinery (Fig. 6*D*).

To confirm the presence of translocation events involving *MLL* within these populations of treated cells, DNA from the IPCR products identified 6–8 h after irradiation was cloned into a pCR4-Topo vector, transformed in DH5$\alpha$ bacteria, and sequenced. Of the 59 clones thus analyzed after irradiation, 5 (8.4%) linked *MLL* to unique sequences (Table 1). Of 20 clones extracted from the anti-CD95-treated populations, 3 of 20 (15%) contained translocations, confirming the ability of the apoptotic effector process itself to generate DNA translocations (Table 1). NHEJ repair is facilitated by the presence of short regions of complementary sequence that align the broken ends before the completion of the ligation process (27). All but two of the translocation breakpoints contained short tracts of homologous sequence at the breakpoint (Table 1), indicating that NHEJ was the most likely mechanism involved (2). In addition, two of the translocations included repetitive DNA as LINE sequences: we have shown previously that such DNA tracts are targets for apoptotic cleavage (28).

These data demonstrate the accumulation of critical components of the NHEJ machinery at the *MLL* breakpoint, its involvement in a NHEJ-mediated DNA break-rejoining event, and the generation of translocations without prior genotoxic damage. Others have reported that components of the NHEJ pathway and its repair function contribute to genomic stability and suppress translocations (29). This is not in conflict with the data presented here because the MLL target site is subject to repetitive breakage and rejoining cycles, increasing the possibility of errors.

The mechanism whereby the apoptotic effector cascade leads to DNA cleavage has been studied extensively (20). Contrary to earlier expectations, the cleavage of DNA during apoptosis is not essential for the creation of the apoptotic phenotype. Certain cells, predominantly cells of lymphoid origin, rapidly cleave DNA to both large (50 kb and greater) and small (internucleosomal) fragments, although others such as fibroblasts do not (30). This process has been linked to the operation of a specific nuclease, the CAD, which is normally kept inactive by binding to its inhibitor, ICAD (31). The specific targeting of *MLL* exon 12 region by nucleases of the apoptotic effector system may be related to the presence of scaffold or matrix attachment regions within this region of *MLL* (6). We have shown previously that these sites of DNA attachment are a target for early apoptotic cleav-

Table 1 *MLL translocation breakpoint junctions identified in TK6 cells, 6 (F) or 8 h (R) after apoptotic stimuli*

| Trigger | *MLL* Break site | Cloned length (bp) | *MLL* (11q23) partner | Break Junction |
|---|---|---|---|---|
| R | 6556 | 230 | Ch 3 | Ch 3-CCTTTTAATCC**TT**CACAATATAAGG<br>Bkpt-ATATTTATT**TT**CACAATATAAGG<br>MLL-ATATTTATT**TT**GTTACTTTC |
| R | 6800 | 36 | Ch 3 | Ch 3-TAAGTTCC**CAACAGACTT**GTCCTGCT<br>Bkpt-TAAGTTCC**CAACAGACTT**GGCAATAC<br>MLL-GAAGGGCTCA**CAACAGACTT**GGCAATA |
| R | 6543 | 167 | Ch 1 | Ch 1-GGTGACTGGCGGTTG**TAC**TTTCTT<br>Bkpt-GGTGACTGGCGGTTC**TAC**AAGATTTAA<br>MLL-CAAAATAAATATAA**TAC**AAGATTTAA |
| R | 6570 | 183 | Ch 17q23 | Ch 17-TCTTGGAGAA**AA**GATCTGGTC<br>Bkpt-TCTTGGAGAA**AA**ATAGAAAGTAACA<br>MLL-ATACCAGTGG**AA**ATAGAAAGTAACA |
| F | 6576 | 519 | Ch 19 | Ch 19-CTCTAA**TTCCACTG**ATCCAAAAAGG<br>Bkpt-CTAAT**TTCCACTG**ATCCAAAAAGG<br>MLL-TCTAAT**TTCCACTG**GTATTACCACTT |
| F | 6772 | 214 | Ch 2 | Ch 2-GACAGAGCGAGACTGTCTCAAAAAA<br>Bkpt-GACAGAGCGAGACGTAAGAACATGGG<br>MLL-ACACAAACTATAGTAAGAACATGGGA |
| F | 6597 | 283 | LINE L1 | LINE L1-TTATTTAAT**ATCT**TTCAA<br>Bkpt-TACTCTGT**ATCT**TTCAA<br>MLL-TACTCTGA**ATCT**CCCGCAA |
| R | 6552 | 258 | Alu - LINE L1 | Alu-LINE-CTTGGCGGTCAGT<br>Bkpt-AATTTAGAACATCTTGGCGGTCAGT<br>MLL-AATTTAGAACATAATATAAATAAA |

Apoptotic stimuli were either 0.5 $\mu$g/ml anti-CD95 antibody (F) or 8 Gy of irradiation (R). Individual breakpoint junctions are shown flanked by germ-line *MLL* (bottom) and the putative translocation partner, where known (top). The boxed sequences in bold indicate regions of microhomology between *MLL* and partner DNA. Cloned length indicates the size of the foreign DNA attached to *MLL,* and break site refers to the position within the 8.3-kb *MLL* germ-line BCR ligated to foreign DNA (33).

age, specifically those containing LINE and short interspersed nucleotide element repetitive DNA (28).

In terms of this study, there are two biologically relevant fates for cells containing site-specific cleavage within the *MLL* BCR after exposure to proapoptotic stimuli; they may either execute apoptosis and die or abort the process and survive. In the latter case, there are at least two possible mechanisms that might lead to cell survival. First, enzymes of the CAD/ICAD type may become active in damaged cells that have not initiated the apoptotic program. This may be a result of direct action of CAD before its association with ICAD or through release of CAD from its inhibitor ICAD molecule by transient caspase 3 activation, nonspecific protease action, or competitive inhibition. In support of this possibility, it has been shown that caspase 3, 6, and 7 may be activated in nonapoptotic T lymphocytes after T-cell receptor engagement (32). Second, DNA cleaved within *MLL* may be joined to other break sites within cells that have activated but are not irreversibly committed to execution of the apoptotic program. This is consistent with data discussed above, where markers of apoptotic cells, such as phosphatidyl serine membrane expression measured by annexin V staining and chromatin cleavage shown by terminal deoxynucleotidyl transferase-mediated nick end labeling staining, are both observed within viable populations of cells (21, 22). In either case, a small fraction of those breaks that undergo translocation may also confer a growth advantage to the affected cell and contribute to leukemogenesis.

These data support the interaction of the NHEJ program with the apoptotic pathway as a novel mechanism whereby translocations are generated in *MLL*. Unlike leukemogenic chromosome rearrangements of unknown origin, translocations mediated by nucleases of the apoptotic pathway, particularly during therapy for existing disease, may be preventable. Thus, agents that promote efficient activation and execution of the chromatin cleavage phase of apoptosis may eliminate those cells that generate inappropriate cycles of DNA breakage and rejoining and have also evaded apoptotic execution.

## REFERENCES


1. Roulston, D., Espinosa, R., III, Nucifora, G., Larson, R. A., Le Beau, M. M., and Rowley, J. D. CBFA2(AML1) translocations with novel partner chromosomes in myeloid leukemias: association with prior therapy. Blood, *92:* 2879–2885, 1998.
2. Reichel, M., Gillert, E., Nilson, I., Siegler, G., Greil, J., Fey, G. H., and Marschalek, R. Fine structure of translocation breakpoints in leukemic blasts with chromosomal translocation t(4;11): the DNA damage-repair model of translocation. Oncogene, *17:* 3035–3044, 1998.
3. Gu, Y., Cimino, G., Alder, H., Nakamura, T., Prasad, R., Canaani, O., Moir, D. T., Jones, C., Nowell, P. C., Croce, C. M., and Canaani, E. The (4;11)(q21;q23) chromosome translocations in acute leukemias involve the VDJ recombinase. Proc. Natl. Acad. Sci. USA, *89:* 10464–10468, 1992.
4. Marschalek, R., Greil, J., Lochner, K., Nilson, I., Siegler, G., Zweckbronner, I., Beck, J. D., and Fey, G. H. Molecular analysis of the chromosomal breakpoint and fusion transcripts in the acute lymphoblastic SEM cell line with chromosomal translocation t(4;11). Br. J. Haematol., *90:* 308–320, 1995.
5. So, C. W., Ma, Z. G., Price, C. M., Dong, S., Chen, S. J., Gu, L. J., So, C. K., Wiedemann, L. M., and Chan, L. C. *MLL* self fusion mediated by Alu repeat

homologous recombination and prognosis of AML-M4/M5 subtypes. Cancer Res., *57:* 117–122, 1997.
6. Broeker, P. L., Super, H. G., Thirman, M. J., Pomykala, H., Yonebayashi, Y., Tanabe, S., Zeleznik-Le, N., and Rowley, J. D. Distribution of 11q23 breakpoints within the *MLL* breakpoint cluster region in *de novo* acute leukemia and in treatment-related acute myeloid leukemia: correlation with scaffold attachment regions and topoisomerase II consensus binding sites. Blood, *87:* 1912–1922, 1996.
7. Strissel, P. L., Strick, R., Tomek, R. J., Roe, B. A., Rowley, J. D., and Zeleznik-Le, N. J. DNA structural properties of AF9 are similar to *MLL* and could act as recombination hot spots resulting in *MLL*/AF9 translocations and leukemogenesis. Hum. Mol. Genet., *9:* 1671–1679, 2000.
8. Richardson, C., and Jasin, M. Frequent chromosomal translocations induced by DNA double-strand breaks. Nature (Lond.), *405:* 697–700, 2000.
9. Chu, G. Double strand break repair. J. Biol. Chem., *272:* 24097–24100, 1997.
10. Tsukamoto, Y., and Ikeda, H. Double-strand break repair mediated by DNA end-joining. Genes Cells, *3:* 135–144, 1998.
11. Critchlow, S., and Jackson, S. DNA end-joining: from yeast to man. Trends Biochem. Sci., *10:* 394–398, 1998.
12. Kanaar, R., Hoeijmakers, J. H. J., and van Gent, D. C. Molecular mechanisms of DNA double-strand break repair. Trends Cell. Biol., *8:* 483–489, 1998.
13. Weaver, D. What to do at an end: DNA double-strand break repair. Trends Genet., *11:* 388–392, 1995.
14. Hiom, K., Melek, M., and Gellert, M. 70 DNA transposition by the RAG1 and RAG2 proteins: a possible source of oncogenic translocations. Cell, *94:* 463–470, 1998.
15. DiBiase, S. J., Zeng, Z. C., Chen, R., Hyslop, T., Curran, W. J., Jr., and Iliakis, G. DNA-dependent protein kinase stimulates an independently active, nonhomologous, end-joining apparatus. Cancer Res., *60:* 1245–1253, 2000.
16. Stanulla, M., Wang, J., Chervinsky, D. S., Thandala, S., and Aplan, P. D. DNA cleavage within the *MLL* breakpoint cluster region is a specific event which occurs as part of higher-order chromatin fragmentation during the initial stages of apoptosis. Mol. Cell. Biol., *17:* 4070–4079, 1997.
17. Aplan, P. D., Chervinsky, D. S., Stanulla, M., and Burhans, W. C. Site-specific DNA cleavage within the *MLL* breakpoint cluster region induced by topoisomerase II inhibitors. Blood, *87:* 2649–2658, 1996.
18. Boyd, K. E., Wells, J., Gutman, J., Bartley, S. M., and Farnham, P. J. c-Myc target gene specificity is determined by a post-DNA binding mechanism. Proc. Natl. Acad. Sci. USA, *95:* 13887–13892, 1998.
19. Ochman, H., Gerger, A. S., and Hartl, D. L. Genetic applications of an inverse polymerase chain reaction. Genetics, *120:* 621–623, 1988.
20. Robertson, J. D., Orrenius, S., and Zhivotovsky, B. Review: nuclear events in apoptosis. J. Struct. Biol., *129:* 346–358, 2000.
21. Geske, F. J., Nelson, A. C., Lieberman, R., Strange, R., Sun, T., and Gerschenson, L. E. DNA repair is activated in early stages of p53-induced apoptosis. Cell Death Differ., *7:* 393–401, 2000.
22. Hammill, A. K., Uhr, J. W., and Scheuermann, R. H. Annexin V staining due to loss of membrane asymmetry can be reversible and precede commitment to apoptotic death. Exp. Cell. Res., *25:* 16–21, 1999.
23. Boulton, S., Kyle, S., Yalcintepe, L., and Durkacz, B. Wortmannin is a potent inhibitor of DNA double strand break but not single strand break repair in Chinese hamster ovary cells. Carcinogenesis (Lond.), *17:* 2285–2290, 1996.
24. Okayasu, R., Suetomi, K., and Ullrich, R. Wortmannin inhibits repair of DNA double-strand breaks in irradiated normal human cells. Radiat. Res., *149:* 440–445, 1998.
25. Walczak, H., and Krammer, P. H. The CD95 (APO-1/Fas) and the TRAIL (APO-2L) apoptosis systems. Exp. Cell. Res., *256:* 58–66, 2000.
26. Zhen, W., Denault, C. M., Loviscek, K., Walter, S., Geng, L., and Vaughan, A. T. The relative radiosensitivity of TK6 and WI-L2-NS lymphoblastoid cells derived from a common source is primarily determined by their p53 mutational status. Mutat. Res., *346:* 85–92, 1995.
27. Roth, D. B., and Wilson, J. H. Nonhomologous recombination in mammalian cells: role for short sequence homologies in the joining reaction. Mol. Cell. Biol., *6:* 4295–4304, 1986.
28. Khodarev, N. N., Bennett, T., Shearing, N., Sokolova, I., Koudelik, J., Walter, S., Villalobos, M., and Vaughan, A. T. LINE L1 retrotransposable element is targeted during the initial stages of apoptotic DNA fragmentation. J. Cell. Biochem., *79:* 486–495, 2000.
29. Ferguson, D. O., Sekiguchi, J. M., Chang, S., Frank, K. M., Gao, Y., DePinho, R. A., and Alt, F. W. The nonhomologous end-joining pathway of DNA repair is required for genomic stability and the suppression of translocations. Proc. Natl. Acad. Sci. USA, *97:* 6630–6633, 2000.
30. Nagata, S. Apoptotic DNA fragmentation. Exp. Cell. Res., *256:* 12–18, 2000.
31. Sakahira, H., Enari, M., and Nagata, S. Cleavage of CAD inhibitor in CAD activation and DNA degradation during apoptosis. Nature (Lond.), *391:* 96–99, 1998.
32. Alam, A., Cohen, L. Y., Aouad, S., and Sekaly, R-P. Early activation of caspases during T lymphocyte stimulation results in selective substrate cleavage in nonapoptotic cells. J. Exp. Med., *190:* 1879–1890, 1999.
33. Gu, Y., Alder, H., Nakamura, T., Schichman, S. A., Prasad, R., Canaani, O., Saito, H., Croce, C. M., and Canaani, E. Sequence analysis of the breakpoint cluster region in the ALL-1 gene involved in acute leukemia. Cancer Res., *54:* 2326–2330, 1994.